Evaluating VNA post-calibration residual errors using the ripple technique at millimetre wavelengths in rectangular waveguide

C P Eiø and N M Ridler
RF & Microwave Guided Wave Metrology Group, National Physical Laboratory
Email: chris.eio@npl.co.uk or nick.ridler@npl.co.uk

Abstract

This report presents typical values for the sizes of some residual errors that remain after calibrating Vector Network Analysers (VNAs) at millimetre-wave frequencies. The values have been obtained using the ripple technique in three rectangular waveguide sizes covering the frequency range 33 GHz to 110 GHz. The reported values indicate the likely size of these errors that may be found on other VNAs. The values can also be used when evaluating the uncertainty of measurement arising from these errors for such systems.

1. INTRODUCTION

This report contains information for users of Vector Network Analysers (VNAs) on evaluating post-calibration residual errors at millimetre wavelengths in rectangular waveguide. Although there are many potential contributions to the uncertainty budget for a VNA measurement, this report concentrates on two specific components; the residual (or effective) directivity and test port match error terms. The method used to evaluate these components is the ripple technique. This method has been described elsewhere [1], where it has been recommended for use in coaxial line at frequencies up to 33 GHz (i.e. the maximum recommended operating frequency for 3.5 mm precision connectors). This report investigates extending this method by applying it to VNAs operating up to 110 GHz in rectangular waveguide. This has been achieved in three waveguide bands (as described in Appendix A).

Previous work [2] has provided some information on the typical performance of the ripple technique under the conditions specified in [1] (i.e. in coaxial line up to 33 GHz). This work considered effects on the likely size of the error terms due to using different connectors and calibration schemes. This report complements this work by providing similar performance indicators for different rectangular waveguide sizes and calibration schemes at frequencies from 33 GHz to 110 GHz. There is also some additional information relating to the implementation of the ripple technique in rectangular waveguide, namely: i) verifying ripple plots; ii) considering effects due to changing the components used to obtain ripple plots; and, iii) considering effects due to dimensional imperfections in the apertures of the ripple line. Finally, Appendix B presents some typical ripple plots for rectangular waveguide at these frequencies and Appendix C shows the typical contribution to a VNA uncertainty budget due to the residual directivity and test port match error terms.

2. CALIBRATION SCHEMES

The sizes of VNA residual errors differ from one calibration scheme to the next. Therefore typical values for the residual errors have been assessed for four different calibration schemes in each rectangular waveguide size. These calibration schemes were:

- **S**hort – **O**ffset **S**hort – **L**oad (SOSL)
- **S**hort – **O**ffset Short – **L**oad – **O**ffset Load (SOLO)
- **T**hrough – **R**eflect – **L**ine (TRL)
- **L**ine – **R**eflect – **L**ine (LRL)

The SOSL and SOLO schemes are one-port calibration schemes with the advantage that they are relatively quick to perform. They can be extended to provide a full two-port calibration by including a Through connection. The TRL and LRL schemes calibrate both ports simultaneously and therefore provide a full two-port calibration.

3. RESIDUAL ERROR TERMS

Reference [1] gives the following model for voltage reflection coefficient (VRC) measurements:[1]

$$U_{\mathrm{VRC}} = D + T\Gamma + M\Gamma^{2} + R_{\mathrm{VRC}} + S_{21}{}^{2}\Gamma_{\mathrm{L}} \qquad (1)$$

where Γ is the measured VRC (in linear units)
U_{VRC} is the uncertainty in the VRC measurement
D is the residual (or effective) directivity
M is the residual (or effective) test port match
T is the estimated overall effect of tracking and non-linearity
R_{VRC} represents all random contributions (e.g. connection repeatability, etc)
Γ_{L} is the residual (or effective) load match of the other test port (i.e. $\Gamma_{\mathrm{L}} = 0$ for one-port calibration schemes)
S_{21} is the measured transmission (in linear units) of the device under test (i.e. $S_{21} = 0$ for one-port devices)

Note that this report considers only the evaluation of the *D* and *M* terms in the above model.

Reference [1] also gives a model for transmission measurements, but residual directivity and test port match usually play a less significant role in the evaluation of the uncertainty in transmission measurements and so this is not considered further in this report.[2]

[1] All terms in this model are in fact complex-valued quantities. However, only the magnitude of these quantities is considered in this report.

[2] The residual directivity and test port match will, however, contribute to the uncertainty due to mismatch when making transmission measurements.

3.1 Assessment of residual directivity

The assessment of residual directivity in millimetre wavelength waveguide sizes is essentially the same as that described in [1]; connect a line of suitable length[3] to the measurement reference plane and terminate the line with a suitable low reflecting device (i.e. a 'near-matched' load). Measure linear VRC and display as a function of frequency.

The display should show a discernable 'ripple' superimposed on the VRC plot of the load itself. Appendix B gives some examples of typical ripple traces that were achieved during this investigation. The (maximum) residual directivity, D, is determined by taking the maximum adjacent peak-to-trough amplitude, Δ_{dir}, and applying it to the following formula:

$$D = \frac{\Delta_{dir}}{2} \tag{2}$$

The plot also gives an indication of the variation of the residual directivity with frequency. The residual directivity may not necessarily be worse at the higher frequencies. However, one would normally expect the residual directivity to be quite similar across the whole waveguide band. Therefore, in general, the value D can be used to summarise the residual directivity across the full waveguide band.

Values of D will vary from one calibration scheme to another (due to assumptions implicit in the calibration scheme) and also from one waveguide band to another (due mainly to changes in the physical size of the waveguide). Values achieved from the investigations presented in this report are summarised in Table 1.

Table 1: Typical ranges for D for each calibration scheme and waveguide size

Calibration scheme	WG 23	WG 25	WG 27
SOSL	0.003 to 0.006	0.001 to 0.002	0.006 to 0.008
SOLO	0.003 to 0.004	0.001 to 0.002	0.005 to 0.007
TRL	0.002 to 0.003	0.001 to 0.002	0.005 to 0.006
LRL	0.001 to 0.003	0.001 to 0.002	0.005 to 0.006

3.2 Assessment of residual test port match

The procedure for determining the residual test port match is the same as that used to determine the residual directivity except that a short-circuit is used to terminate the line. The VNA again displays a ripple trace (using linear magnitude units), this time close to VRC = 1. However, the VRC may be appreciably less than unity due to losses in the line used to produce the ripple trace. The (maximum) residual test port match, Δ_{tpm}, is derived in a similar manner as Δ_{dir}, i.e. by taking the maximum adjacent peak-to-trough value and applying it to the following formula:

$$M = \frac{\Delta_{tpm}}{2} \tag{3}$$

[3] The length of line used relates directly to the number of ripples that are produced. The longer the line, the more ripples that are produced. A greater number of ripples gives more information about the residual error term as a function of frequency. Therefore, a relatively long length of line should be used so that sufficient ripples are produced. (For example, lines of length 50 mm and 100 mm were used during the ripple assessments presented in this report.)

As before, the plot also gives an indication of the variation of the residual test port match with frequency. The losses in the line will be greater at the lower frequencies, so the magnitude of the VRC observed at the measurement plane will generally increase with frequency. See Appendix B for some typical plots that were produced during this investigation. Values obtained for *M* are also summarised in Table 2.

Table 2: Typical ranges for *M* for each calibration scheme and waveguide size

Calibration scheme	WG 23	WG 25	WG 27
SOSL	0.007 to 0.013	0.004 to 0.007	0.012 to 0.020
SOLO	0.005 to 0.006	0.003 to 0.006	0.005 to 0.010
TRL	0.004 to 0.007	0.001 to 0.002	0.003 to 0.004
LRL	0.004 to 0.007	0.001 to 0.002	0.003 to 0.004

3.3 Observations

Generally, for a given waveguide size, the two-port calibration schemes (TRL and LRL) produce smaller residual error terms (for both *D* and *M*) than the one-port schemes (SOSL and SOLO). Of the one-port schemes, SOLO generally produces smaller residual error terms than SOSL.

In most cases, for each calibration scheme in each waveguide size, $M > D$. However, since the uncertainty contribution due to *M* in equation (1) is obtained by multiplying by Γ^2, this contribution only becomes apparent when measuring relatively large values of Γ.

There is significantly more variation in values of *M* between different calibration schemes and waveguide sizes than there is in the values of *D*.

It is interesting to note that the lowest values of *D* and *M* are obtained in WG 25, not WG 23 as one might expect. The reasons for this are generally unknown; these reasons could include (but are not limited to) mechanical construction of the waveguides or differences due to measurement system set up.[4]

4. FURTHER CONSIDERATIONS

4.1 Verifying 'true' ripple plots

Reference [1] gives an expression for the periodicity, Δf, of a ripple plot in coaxial line as $\Delta f = c/2L$, where *L* is the length of the coaxial ripple line and *c* is the speed of the electromagnetic wave. (For the purposes of such a calculation, it is acceptable to assume that *c* represents the speed of light in vacuum, i.e. approximately 3×10^8 m.s^{-1}.) This is a very useful expression as it enables users to verify easily whether an observed ripple is actually being produced by the ripple line and not by other components that might be causing significant unwanted discontinuities, etc, elsewhere within the measurement system. However, since, for any given frequency, the wavelength in rectangular waveguide is longer than in coaxial line, this equation requires modification.

[4] The measurement set up for WG 23 was slightly different to that for WG 25 and WG 27. The WG 23 system was derived from a coaxial test set using coaxial-to-waveguide adaptors. The WG 25 and WG 27 systems used dedicated millimetre-wave modules and controllers.

An estimate of ripple periodicity in rectangular waveguide, Δf_{wg}, at frequencies in the middle of the waveguide band (where the wavelength is approximately 1.3 times longer, at the same given frequency, than in coaxial line) is given by:

$$\Delta f_{wg} \approx \frac{c}{1.3 \times 2L} \approx \frac{c}{2.6L} \tag{4}$$

Also, since rectangular waveguide is dispersive, the ripple trace will not have a constant periodicity throughout the band. The period of the ripple will be shorter towards the minimum frequency of the band and longer towards the maximum frequency of the band. (This does not depend on the waveguide size – it is therefore expected to be applicable in other rectangular waveguide sizes.)

NOTE: When using equation (4), the length of 'line' relates to the length of transmission line between the VNA's measurement reference plane and the position of the terminating element (i.e. either the metallic sheet of the short-circuit or the resistive element of the load). This length should therefore include any line length present in the device containing the terminating element. For example, this could be an offset length in an offset short-circuit or the (inevitable) length of line separating a resistive load element and the load's flange/connector reference plane.

4.2 Effects due to interchanging components used to obtain ripple plots

Some previous work [3] has looked at the effects of interchanging the components used to perform ripple assessments in coaxial line to 18 GHz. Therefore, a complementary investigation has been undertaken in rectangular waveguide from 75 GHz to 110 GHz. The same (SOSL) calibration was used throughout the investigation. A series of ripple assessments of *D* and *M* were made on this calibration, each time changing one of the components – i.e. the load, short-circuit or line – used to perform the assessment. A total of three different loads, short-circuits and lines were used. Each time a different component was used, the change in observed *D* and *M* was noted. These values are summarised in Table 3.

Table 3: Maximum changes in *D* and *M* due to changing the ripple components

Component changed	**Maximum change in *D***	**Maximum change in *M***
Load	0.003	N/A
Short-circuit	N/A	0.001
Line	0.004	0.002

This table shows that the choice of components used to evaluate the residual directivity, *D*, (i.e. the load and line) can have a significant effect on the value obtained for *D* (compared with the ranges for *D* given in Table 1). However, the choice of components used to evaluate the residual test port match, *M*, (i.e. the short-circuit and the line) has a much less effect on the value obtained (compared with the ranges for *M* given in Table 2).

4.3 Effects due to dimensional imperfections in the ripple line

Reference [1] contains a discussion on the effects of the dimensional tolerances of the line used to perform ripple assessments in coaxial line. (For coaxial line, these dimensions are the diameters of the centre and outer conductors of the line.) Therefore, a similar consideration

can be made for rectangular waveguide – specifically, relating to the dimensional tolerances of the waveguide aperture size.

For example, a typical manufacturer's specification for the tolerances of the dimensions of a waveguide aperture is 10 μm, for precision waveguide sections in the sizes discussed in this report.[5] Reference [4] gives tables of maximum VRCs generated by dimensional tolerances in waveguide apertures.[6] Table 4 contains values derived from [4] for a 10 μm tolerance in the aperture height and width of the three waveguide sizes considered in this report. In each case, the VRCs due to both height and width dimensional tolerances have been converted to equivalent standard uncertainties (by dividing by $\sqrt{3}$). These are then combined (using the root-sum-squared approach) to obtain a combined standard uncertainty in VRC generated by an overall waveguide tolerance of 10 μm (in both dimensions).

Table 4: Values of standard uncertainty linear VRC due to a 10 μm waveguide flange tolerance

Aperture dimension	WG 23	WG 25	WG 27
Height	0.001 0	0.001 6	0.002 3
Width	0.000 9	0.001 3	0.001 8
Combined height and width	0.001 3	0.002 1	0.002 9

The above VRC values indicate the size of a systematic error in defining zero reflection using a waveguide line, e.g. to define the notional characteristic impedance of the waveguide. This is essentially the role played by a ripple line. These values can be used in an uncertainty budget for VNA measurements where the residual directivity and test port match have been assessed using the ripple technique.

5. CONCLUSIONS

This report has presented some typical values for the residual directivity and test port match for a calibrated VNA in rectangular waveguide at millimetre-wave frequencies. Values have been given for each of three waveguide sizes covering the frequency range 33 GHz to 110 GHz. In each size, the effects on the sizes of these values due to four commonly used calibration techniques have been investigated.

In general, for a given calibration technique, the size of the residual error terms are quite similar for each of the waveguide sizes investigated here.[7] However, there is significant variation in the size of the residual error terms with type of calibration technique. The largest residual errors occur when using the SOSL technique. This is followed by the SOLO technique. Finally, the smallest residual error terms occur when using the TRL and LRL techniques. Generally, values of D are smaller than M, and the variability in determining M is larger than in determining D.

[5] This value of 10 μm was substantiated by measuring the mechanical dimensions (i.e. the width and height) of the apertures of the three ripple lines used in section 4.2. The dimensions of all these lines were found to be within 10 μm of their nominal values.

[6] These VRC values were checked against values generated using an electromagnetic simulation software package, called CST Microwave Studio® [5]. The values obtained from these two independent methods generally showed good agreement.

[7] It is interesting to note that, for the investigation reported here, the WG 25 residual error terms were found to be smaller than the other waveguide sizes. The reasons for this are not yet fully understood.

It is expected that the above conclusions (along with the values presented in Tables 1 and 2) will apply to other calibrated VNAs in these waveguide sizes. This information is therefore likely to be useful as a guide to assessing any other such systems.

Finally, in certain applications, it may be necessary to consider a contribution to the overall VNA uncertainty budget due to the dimensional quality of the ripple line (i.e. the tolerance of the waveguide aperture of the line). Under such circumstances, it may be appropriate to obtain traceable dimensional measurements (e.g. the aperture height and width) of the line.

6. REFERENCES

[1] "EA Guidelines on the evaluation of Vector Network Analysers (VNA)", *European co-operation for Accreditation*, Publication Reference EA-10/12, May 2000.

[2] N M Ridler and C Graham, "Some typical values for the residual error terms of a calibrated vector automatic network analyser (ANA)", *BEMC'99 - 9th International Conference on Electromagnetic Measurement*, Conference Digest pp 45/1 – 45/4, Brighton Metropole Hotel, 2 – 4 November 1999.

[3] A G Morgan and N M Ridler, "Investigating the effects of interchanging components used to perform 'ripple' assessments on calibrated vector network analysers", *ANAMET Report 029*, August 2000.

[4] D J Bannister, E J Griffin and T E Hodgetts, "On the dimensional tolerances of rectangular waveguide for reflectometry at millimetric wavelengths", *NPL Report DES 95*, September 1989.

[5] Information on CST Microwave Studio® can be found at the Computer Simulation Technology web-site, www.cst.de.

APPENDIX A: Waveguide descriptions

Descriptions of the three waveguide sizes used for the investigations in this report are given in Table A1. These descriptions are based on information from several sources, including [A1]. Dimensions *a* and *b* are the internal dimensions of the waveguide as shown in Figure A1. Elsewhere in the report, dimension *a* is referred to as the waveguide width and dimension *b* as the waveguide height.

Table A1: Waveguide sizes used in the investigation

Designation			Typical lower frequency (GHz)	Typical upper frequency (GHz)	*a* (mm)	*b* (mm)
UK	IEC	EIA				
WG 23	R 400	WR 22	33	50	5.690	2.845
WG 25	R 620	WR 15	50	75	3.759	1.880
WG 27	R 900	WR 10	75	110	2.540	1.270

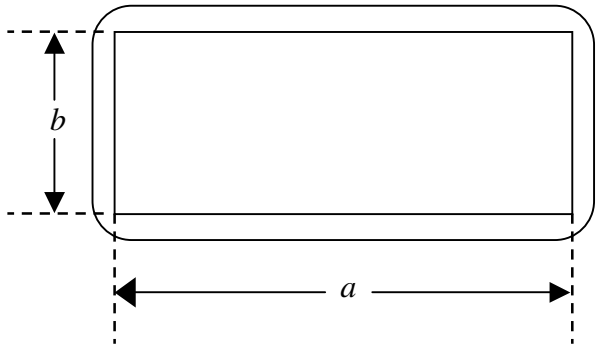

Figure A1: Waveguide aperture showing dimensions *a* and *b*

Reference

[A1] "Hollow metallic waveguides – Part 2: Relevant specifications for ordinary rectangular waveguides", *International Standard IEC 60153-2*, 2nd edition, 1974.

APPENDIX B: Typical ripple plots

This appendix contains a selection of ripple plots obtained during the investigations described in this report. The plots are intended for illustrative purposes only (i.e. to show typical ripple plot sizes and shapes, etc). The shape of other ripple plots (obtained using different equipment, under different circumstances, etc) is likely to be significantly different from the plots presented here.

In WG 23, only plots showing residual directivity and test port match are shown for SOSL calibrations. In WG 25, only plots showing residual directivity and test port match are shown for SOLO calibrations. The plots obtained for TRL and LRL calibrations are often very similar. Therefore, only plots for TRL calibrations are shown here (obtained in WG 27).

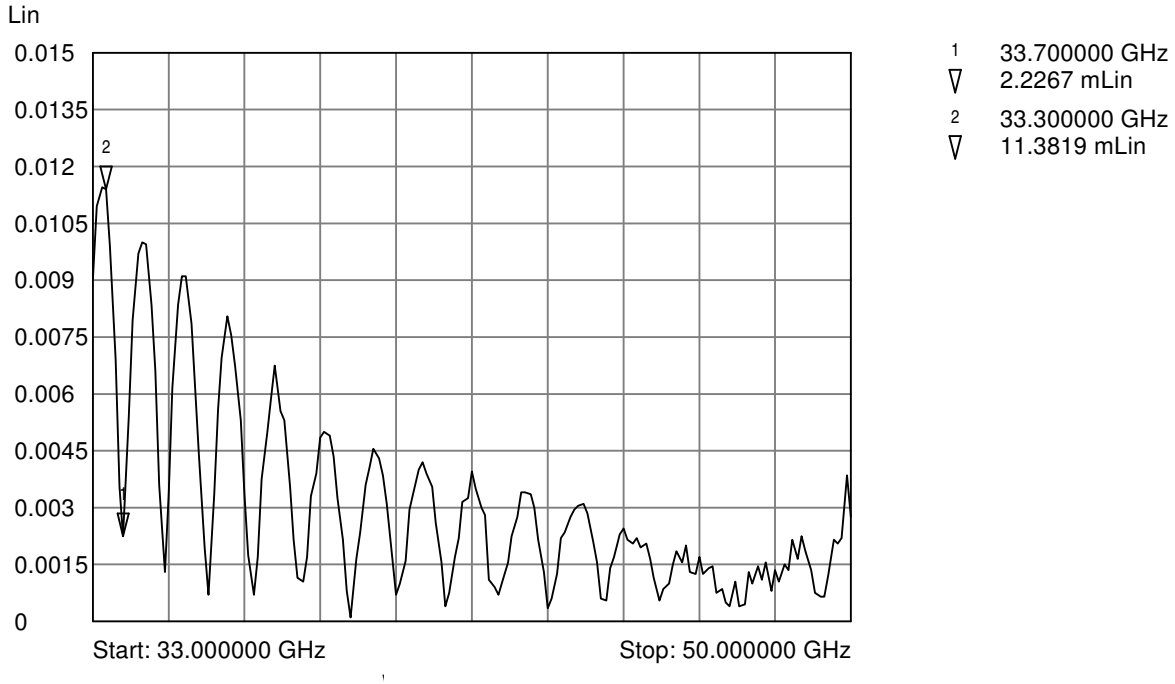

Figure B1: A residual directivity ripple plot observed in WG 23 following a SOSL calibration.

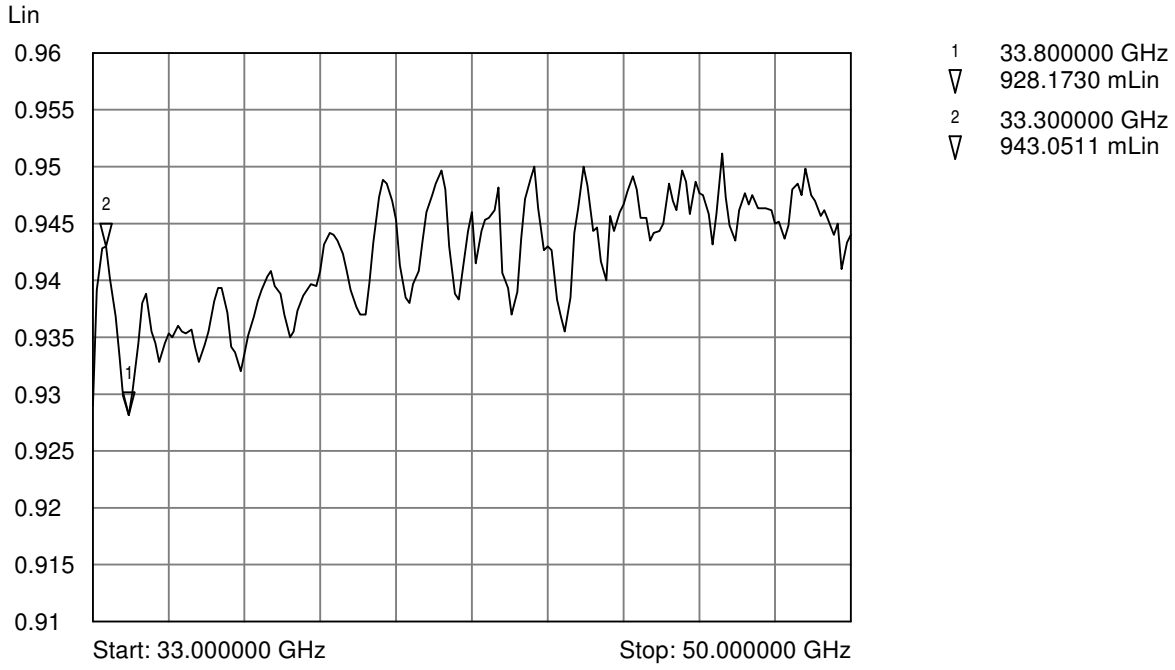

Figure B2: A residual test port match ripple plot observed in WG 23 following a SOSL calibration.

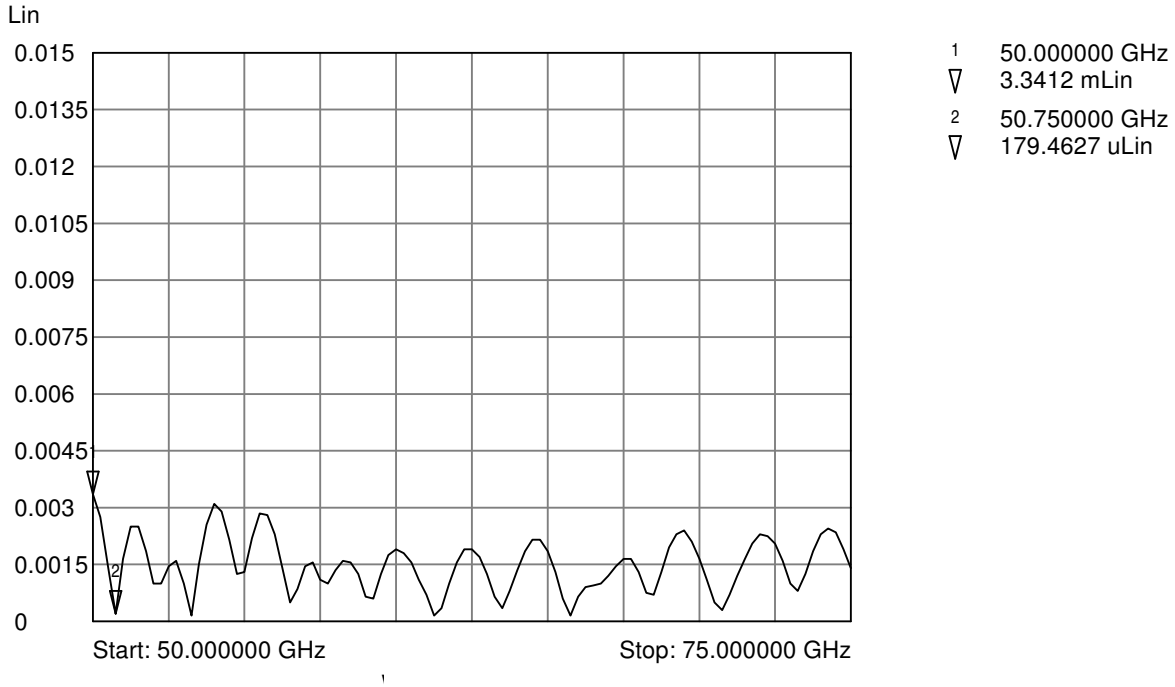

Figure B3: A residual directivity ripple plot observed in WG 25 following a SOLO calibration.

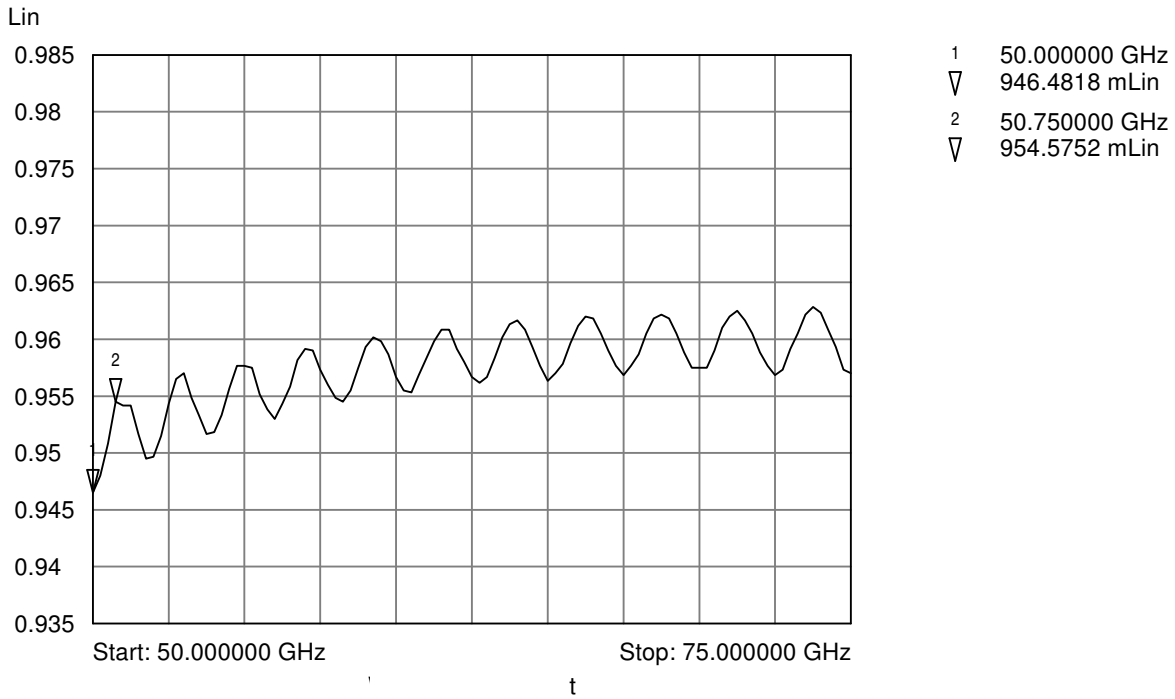

Figure B4: A residual test port match ripple plot observed in WG 25 following a SOLO calibration.

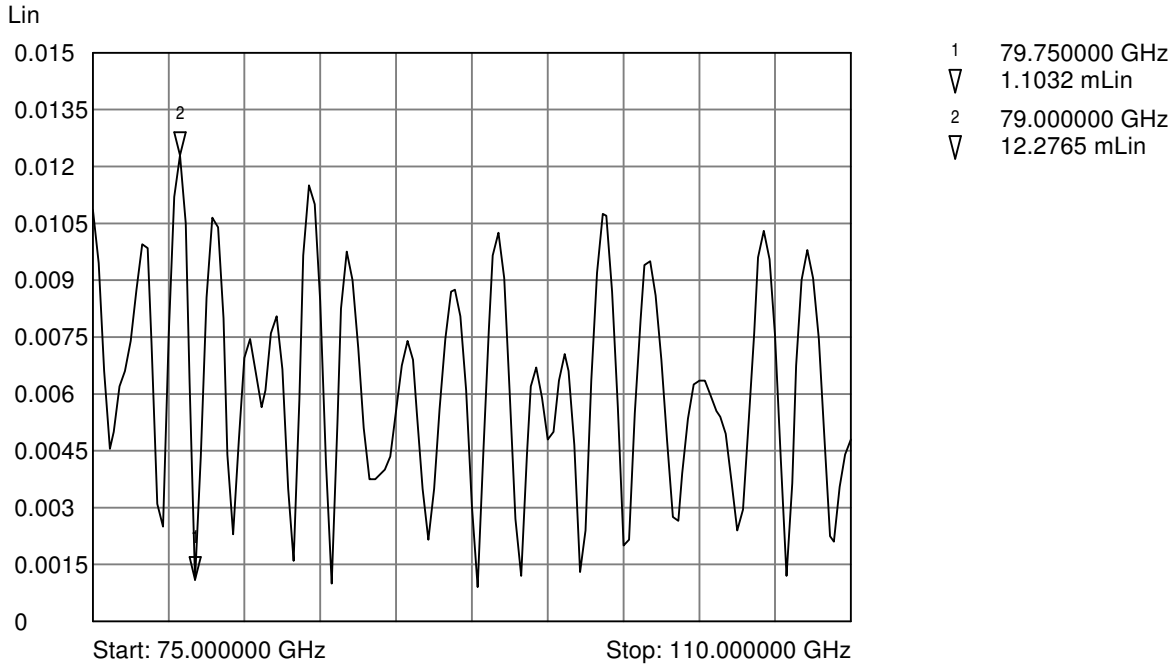

Figure B5: A residual directivity ripple plot observed in WG 27 following a TRL/LRL calibration.

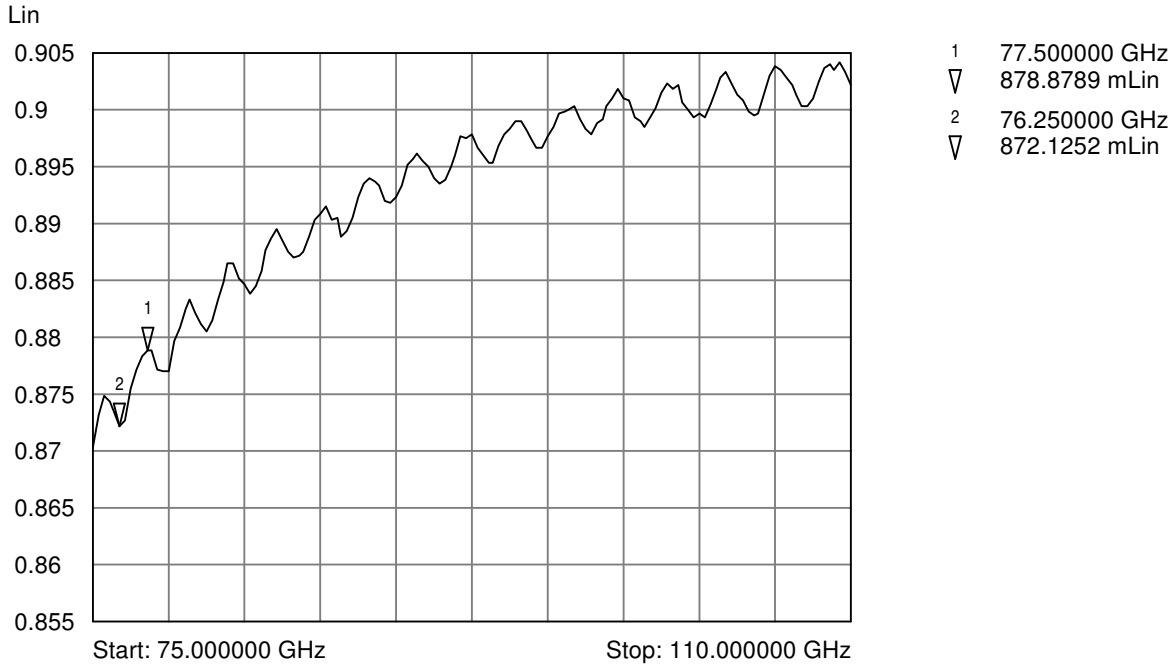

Figure B6: A residual test port match ripple plot observed in WG 27 following a TRL/LRL calibration.

APPENDIX C: Typical contributions to an uncertainty budget for VRC measurements due to residual directivity and test port match

This appendix shows typical values for combined standard uncertainty (for VRC measurements ranging from 0 to 1) due to residual directivity, *D*, and test port match, *M*. To do this, typical values for *D* and *M* have been derived from the midpoint values (suitably rounded) of the ranges for these terms presented in Tables 1 and 2. These midpoint values are shown in Table C1. The values for *D* and *M* for the TRL and LRL are very similar so have therefore been assumed to be the same.

Table C1: Values of *D* and *M* used to evaluate combined standard uncertainty in VRC

	WG 23		WG 25		WG 27	
	D	*M*	*D*	*M*	*D*	*M*
SOSL	0.005	0.010	0.002	0.006	0.007	0.016
SOLO	0.004	0.006	0.002	0.005	0.006	0.008
TRL/LRL	0.002	0.006	0.002	0.002	0.006	0.004

Following the methods given in [1], it is generally assumed that the contributions to uncertainty due to *D* and *M* have U-shaped distributions. Therefore the equivalent standard uncertainties for *D* and *M* are obtained by dividing by √2. Also, since *D* and *M* are generally likely to be correlated, it is good practice to combine these contributions as a linear sum [1]. Figures C1, C2 and C3 show this combined standard uncertainty due to these two terms.

Note that this is not the overall uncertainty of measurement, since many other factors that need to be included in a VNA uncertainty budget [1] have not been included here.

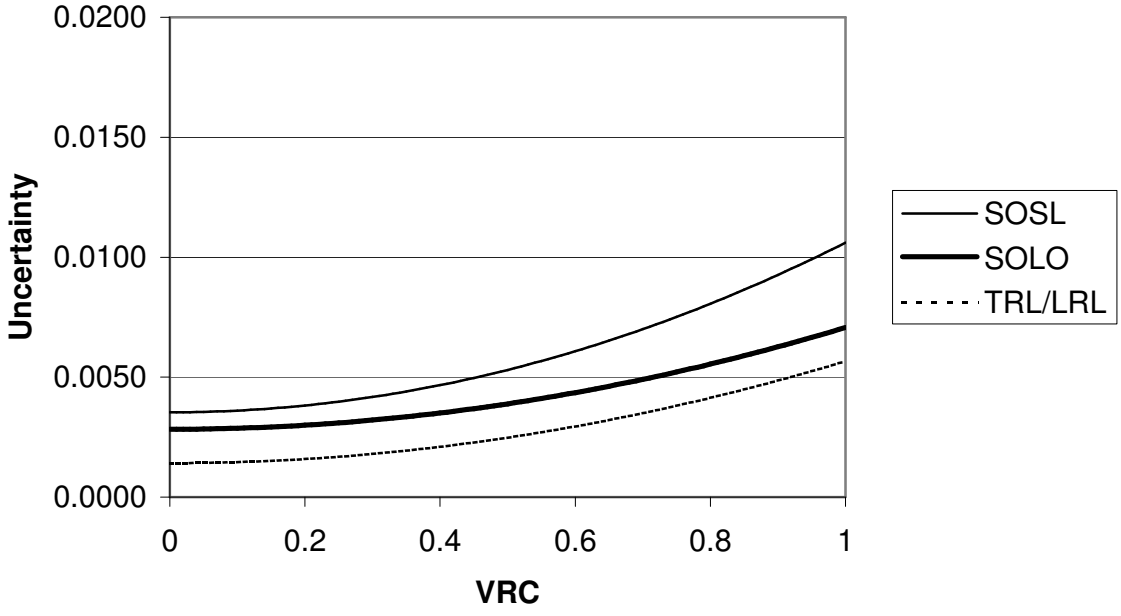

Figure C1 – Typical combined standard uncertainty due to *D* and *M*, as a function of VRC value, in WG 23

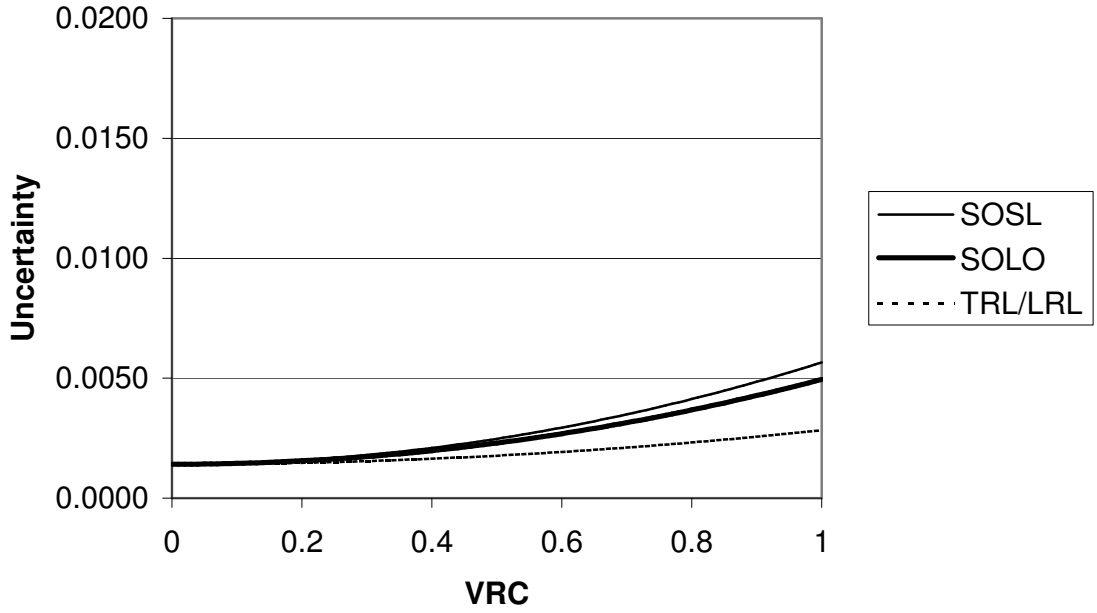

Figure C2 – Typical combined standard uncertainty due to *D* and *M*, as a function of VRC value, in WG 25

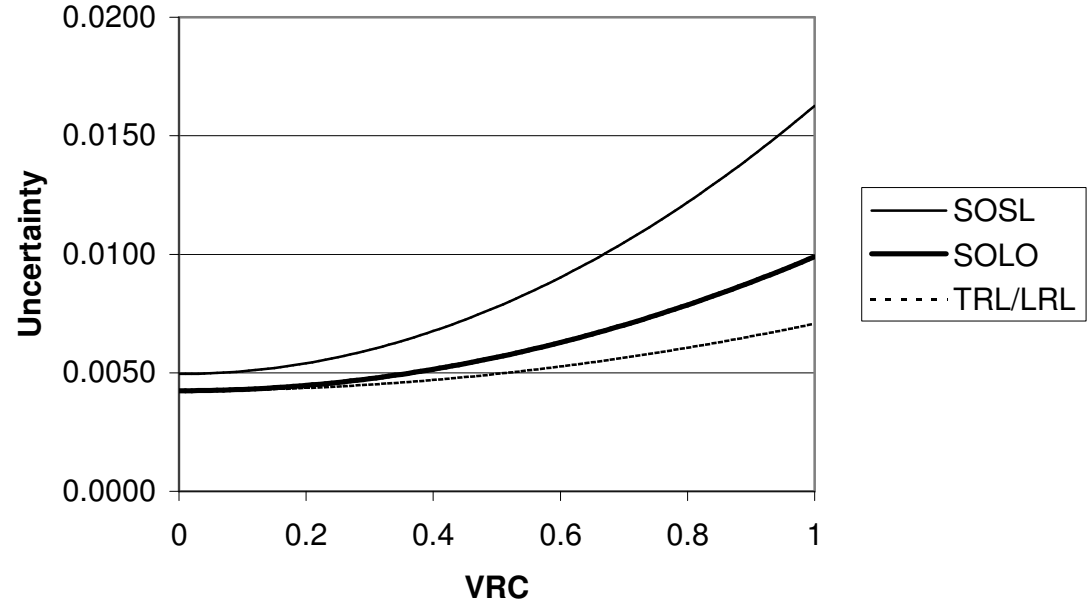

Figure C3 – Typical combined standard uncertainty due to *D* and *M*, as a function of VRC value, in WG 27